18TH WORLD CONFERENCE ON EARTHQUAKE ENGINEERING
WCEE2024
MILAN

MILAN, ITALY
30TH JUNE - 5TH JULY 2024
www.wcee2024.it

RESILIENCE OPTIMIZATION IN WATER DISTRIBUTION NETWORKS: LARGE-SCALE SIMULATION AND RECOVERY PLANNING

O. Kammouh[1], G.P. Cimellaro[2]

[1] Delft University of Technology, Delft, The Netherlands, o.kammouh@tudelft.nl

[2] Politecnico di Torino, Turin, Italy

Abstract: *The ability of a community to respond effectively to emergencies is closely linked to the wellbeing of its infrastructure. Many global infrastructures are outdated, making them particularly vulnerable to natural disasters like earthquakes. In this context, this paper introduces a simulation-based approach to measure and improve the resilience of large-scale Water Distribution Networks (WDN). We evaluate network resilience using two key metrics: the first counts the number of users who lose access to water, and the second quantifies the reduction in total water supply. Both metrics are considered under the assumption that a localized system failure happens when both water pressure and flow rate fall below certain levels. We test the network's performance under various earthquake scenarios, calculating the potential damage through fragility functions that take into account both the network's characteristics and the seismic forces involved. Our model is applied to a simulated community of 900,000 people, revealing significant correlations between the timing of the earthquake, daily water demand, and the material properties of the pipes. Additionally, we present a plan to incorporate a recovery optimization module in future work. This module aims to dynamically prioritize repair tasks based on various constraints like available manpower, equipment, and budget, with the ultimate objective of maximizing the number of residents served with adequate water pressure during the recovery process.*

1. Introduction

Community resilience is largely determined by how quickly and effectively its physical and non-physical systems can recover after a disaster (Ellingwood et al. 2016). While much has been done to evaluate general resilience in communities (Bruneau et al. 2003; Kammouh et al. 2019; Kammouh et al. 2018c), there is a growing focus on specific infrastructure types like transportation (Kammouh et al. 2018a; Nogal and Honfi 2019; Nogal et al. 2016; Nogal et al. 2017), water (Pagano et al. 2019; Soldi et al. 2015), and buildings (Marasco et al. 2018; Zamani Noori et al. 2017). This study focuses on assessing the resilience of Water Distribution Networks (WDN). Although numerous metrics and models have been proposed to evaluate WDN resilience, a universal method has yet to be established. Existing metrics often miss out on capturing dynamic changes in infrastructure function infrastructure (De Iuliis et al. 2019; De Iuliis et al. 2020; Kammouh et al. 2018b). Therefore, we highlight the need for computational models that can examine various aspects of resilience, aiding in scientific applications and decision-making.

For this research, we model a water distribution network in a virtual city, putting a significant emphasis on data gathering, analysis, and network modeling. The virtual WDN is subject to a range of earthquake scenarios, taking into account time-dependent water demand and the uncertain behavior of pipe materials, as assessed through fragility curves. We also explore the impact of different pipe materials on overall system resilience. This model uses two primary resilience metrics: the number of affected residents and the reduction in overall water supply. Our findings reveal that resilience is influenced by factors such as water demand cycles and the timing of earthquake events, as well as the choice of pipe material.

The paper is structured as follows: Section 2 outlines the resilience metrics used in this study. Section 3 discusses the creation of the virtual city and water network modeling. Section 4 focuses on pipe vulnerability and the use of fragility curves. Section 5 describes the earthquake scenarios applied and analyzes the results. Section 6 presents a plan to incorporate a recovery optimization module in future work. Finally, conclusions are drawn in Section 7.

2. Resilience metrics

The effectiveness of a Water Distribution Network (WDN) is evaluated by its ability to meet water demand while maintaining adequate pressure levels. Earthquake-induced damages typically result in a pressure drop, subsequently affecting water supply availability. In this study, we adopt a 24-hour demand cycle based on customer needs within the model. Two key performance metrics are introduced: $F_1(t)$ and $F_2(t)$. $F_1(t)$ quantifies the number of people experiencing water shortage due to low pressure, and $F_2(t)$ assesses the water supply-demand ratio at any given time.

The mathematical representations for $F_1(t)$ and $F_2(t)$ are as follows:

$$F_1(t) = 1 - \frac{\sum_{i=1}^{N} n_e^i(t)}{n_{tot}} \tag{1}$$

where $n^i_e(t)$ represents the number of residents at node i experiencing insufficient pressure (below 40m), n_{tot} denotes the total population, and N is the total number of nodes in the network.

Similarly, the equation for $F_2(t)$ is:

$$F_2(t) = \frac{\sum_{i=1}^{N} Q_{supply,i}(t)}{\sum_{i=1}^{N} Q_{demand,i}(t)} \tag{2}$$

Here, $Q_{supply,i}$ and $Q_{demand,i}$ signify the water supply and demand at node i, respectively. Both variables are time-sensitive.

For both performance metrics, a corresponding resilience index is calculated as the area under each function during a predefined control period, following the methodology presented by Cimellaro et al. 2016:

$$R = \int_{t_1}^{t_2} \frac{F(t)}{T_R} \mathrm{d}t \tag{3}$$

where t_1 is the time of the earthquake's occurrence and t_2 is when the network regains its functionality. In this study, the recovery period is assumed to be 24 hours for both metrics.

3. Model Description, Assumption, and Calibration

The study employs a virtual urban environment, named IDEAL CITY (Fig. 1). The IDEAL CITY encompasses an area of 120 km and houses with approximately 900,000 residents. The city layout is divided into 10 distinct districts, modeled after the real-world city of Turin, Italy. Data and information about the city infrastructure are provided as separate layers in a GIS environment using “ArcGIS” software (ESRI 2011).

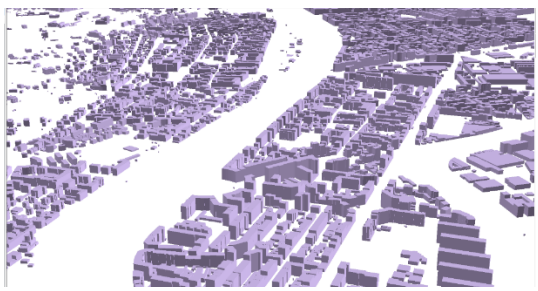

Fig. 1. IDEAL CITY: 3D view using “ArcGIS” software.

The water network analysed in this study is based on the urban water network of the city of Turin. Elevations of the grounds are from Google Maps®. Several assumptions are made to build the water network model. The geometry of the water network is assumed to overlap with the transportation network of the city. The water network model (Fig. 2) is built using the Epanet-Matlab toolkit, which allows controlling Epanet 2.0 using MATLAB® (Eliades). The EPANET-based model comprises various components with the following attributes:

- Pipes: 19,654 ductile iron pipes with a combined length of 1,285,007 meters.
- Roughness Coefficient: A Darcy-Weisbach roughness coefficient of 0.26 mm is assumed for the pipes.
- Nodes: A total of 14,996 nodes are present, each located 1.2 meters below the ground surface.
- Components: The model includes 9 valves, 38 pumps, 19 reservoirs, and 26 storage tanks.
- Ground Elevation: Varies between 207.76 meters and 340.68 meters above sea level.
- Water Sources: The water is primarily sourced from aquifers (82%) and supplemented by rivers and surface water (18%).
- Daily Demand: The average total water demand for the city is 353.38 million litres per day (Ml/day).

The water demand at each node (junction) depends on the number of people who are served by that node. In this work, the nodes are connected to the households and not to the population. Therefore, it is first necessary to find the population density per each unit volume of households, which also depends on the district as the population density is not the same across all districts. This is done as follows:

$$\rho_j \left(people / m^3 \right) = \frac{P_j}{V_j} \tag{4}$$

where ρ_j is the household population density in district j, given in terms of number of people per unit volume of household, P_j is the number of people in district j, and V_j is the total volume of households located in district j.

The water network is considered as a mesh model formed by the pipes' interconnections. Each mesh element (closed shaped) is assigned a water demand based on the total volume of household located inside:

$$Q_{demand,j,w} = \rho_j \cdot \delta \cdot V_w \tag{5}$$

where $Q_{demand,j,w}$ is the water demand in a mesh element w in district j, δ is the city water supply per inhabitant, obtained from the municipality of the city of Turin (315 l/capita/day), V_w is the volume of the households within mesh element w.

The total water demand per mesh element, $Q_{demand,j,w}$, is equally distributed among the adjoining nodes (Fig. 3 (a)). Hence, the water demand at each node, $Q_{demand,i}$, is the sum of the demand contribution from the adjoining mesh elements (Fig. 3 (b)):

$$Q_{demand,i} = \sum_{w=1}^{n_{w,i}} \frac{Q_{demand,j,w}}{n_{i,w}} \tag{6}$$

where $n_{w,i}$ is the number of mesh elements adjoining node i, $n_{i,w}$ is the number of the nodes adjoining mesh w.

For the analysis of the water distribution network (WDN), the formulation is applied in a discrete-time domain assuming time steps of 1 hour.

Fig. 2. The analyzed water distribution network.

Fig. 3. (a) Water demand $Q_{demand,j,w}$ within a mesh element w in district *j*, (b) Water demand at node *i*.

The calibration of a WDN of such a size brings on several difficulties. It is a fundamental issue to ensure an accurate and realistic simulation for both the flow velocity and pressure. The pipes diameters and the positions of the valves, pumps, reservoirs, and tanks have been determined with the following constraints in mind:

$$0.5m/s \leq \text{Velocity} \leq 2m/s \tag{7}$$

$$40m \leq \text{Pressure} \leq 80m \tag{8}$$

Fig. 4 shows the calibrated WDN at the peak hour of water demand. The calibration procedure adopted in this paper is iterative. Future work will be oriented to apply a systematic parametric calibration for large-scale water networks.

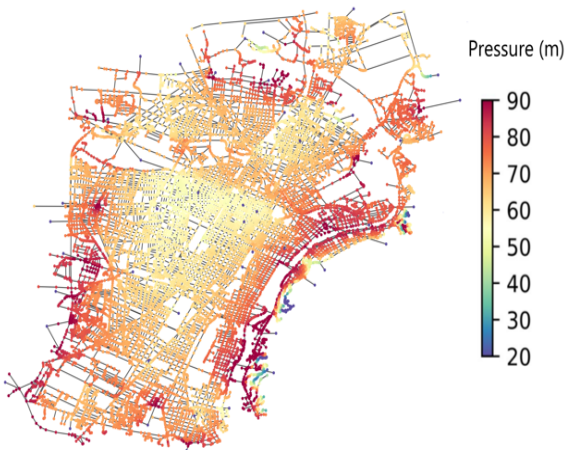

Fig. 4. Water pressure in meters at the first time step of the analysis from the calibrated WDN

4. Vulnerability of the water pipes

The reliability of a water network is strictly connected to the concept of vulnerability of its elements. Herein, the focus is given to the pipe, the most important component in a pipe network, because it is the most challenging part to inspect and

replace, and also its extensive distribution and exposure make it especially vulnerable. The seismic vulnerability of the buried pipelines introduced in the American Lifelines Alliance (ALA 2001) (Eidinger 2001) is adopted in this work. Vulnerability functions are entirely empirical and are based on reported damage from historical earthquakes. Damage is expressed in terms of pipe repair rate, *RR*, defined as the number of repairs per 1,000 m of pipe length exposed to a certain level of seismic intensity The seismic intensity is expressed in terms of Peak Ground Velocity (PGV).

$$RR = 0.00187 \cdot K1 \cdot PGV \tag{9}$$

where *K1* is a coefficient that depends on the pipe material, pipe diameter, joint type, and soil condition. Once the repair rate is known, the failure probability $P_{f,k}$ of a pipeline k is evaluated through the Poisson exponential probability distribution, as follows:

$$P_{f,k} = 1 - e^{-RR \cdot L} \tag{10}$$

where L is the length of pipe, $e^{-RR \cdot L}$ is the probability of zero breaks along the pipe. In this paper, three different values of *K1* are considered in order to investigate the influence of the pipe material on the failure probability $P_{f,k}$: $K1 \in \{0.5;0.8;1\}$. The seismic wave propagation induces strains to the pipes due to the soil-pipe interaction. Strains could produce damage if the pipe strength is exceeded. When pipe damage occurs, the pipe is assumed to break in the middle. Fig. 5 shows the fragility curves generated for the pipes. In the context of this work, only major damage is assumed to cause water leakage.

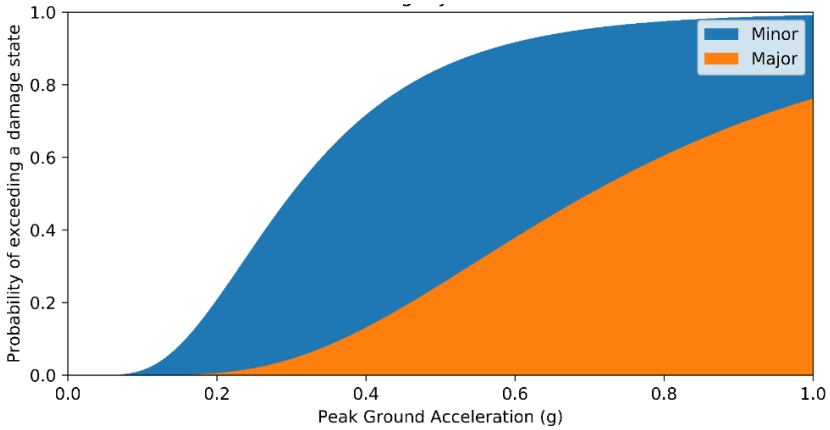

Fig. 5. Fragility function of the water pipes.

Pipe damage is modelled with EPANET2.0® as follows: each damaged pipe is divided into two equal parts. Then, two reservoirs are added at their endpoints in order to simulate the water leakage through the crack (Fig. 6). The reservoirs have a total head equal to the elevation of the middle point of the pipe (assuming that the pipe breaks in the middle). A check valve is inserted so that water only flows towards the reservoirs.

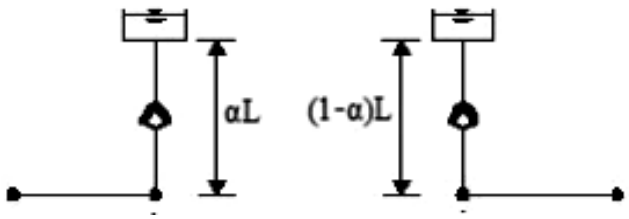

Fig. 6. Pipe break simulation in EPANET 2.0.

A demand-driven analysis (DDA) is carried out in a standard manner using the software EPANET. The problem with DDA is that it fixes the demands at the nodes. However, in the case of pipe damage, the pressure at some nodes drops, and this affects the water supply. Thus, a pressure-driven analysis PDA is needed to account for the dependence of water supply on pressure. To do so, a standard DDA is first performed. Then, nodes with pressure below the value required to satisfy the demand are converted into Emitter nodes. An Emitter is a node whose demand is proportional to a fractional power of the pressure, according to the following equation:

$$Q_{\text{supply},i} = C_i (H_i - z_i)^{\alpha} = C_i \times p_i^{\alpha} \tag{11}$$

where C_i is its corresponding emitter coefficient, H_i is the actual total head of node i, z_i is its elevation, p_i is the actual pressure of the node, and α is the emitter exponent (0.5 if no other information is available). The emitter coefficient is evaluated as follows:

$$C_i = \frac{Q_{demand,i}}{(H_{r,i} - z_i)^{\alpha}} = \frac{Q_{demand,i}}{p_{r,i}^{\alpha}} \tag{12}$$

where $H_{r,i}$ and $p_{r,i}$ are the total head and the pressure required to satisfy $Q_{demand,i}$, respectively. In this work, 20 m of water column is considered as the minimum value to satisfy the demand at any node. The model is run again with the emitters inserted. The PDA procedure is applied during the breakage. Three cases can occur:

- If $Q_{supply,i} \leq 0$, the actual flow at the node is set to zero,
- If $0 \leq Q_{supply,i} \leq Q_{demand,i}$, the actual flow is set equal to $Q_{supply,i}$;
- If $Q_{supply,i} \geq Q_{demand,i}$, the actual flow is set equal to $Q_{demand,i}$.

5. Event scenarios and results

Resilience is a dynamic quantity characterized by a lack of certainty. Uncertainties are crucial both for risk management and resilience analysis (Bozorgnia and Bertero 2004). To study the uncertainty, a Monte Carlo approach is applied to generate a large number of simulations using a Matlab code provided by (Fragiadakis et al. 2012). The code requires pipes diameters, pipes lengths, start and end nodes, and pipes failure probabilities. The earthquake *El centro* that hit the Imperial Valley in south-eastern Southern California near the international border of the United States and Mexico with a magnitude of 6.9 is considered in the analysis. Fig. 7 shows the earthquake epicentre and the Peak Ground Acceleration distribution considering the attenuation.

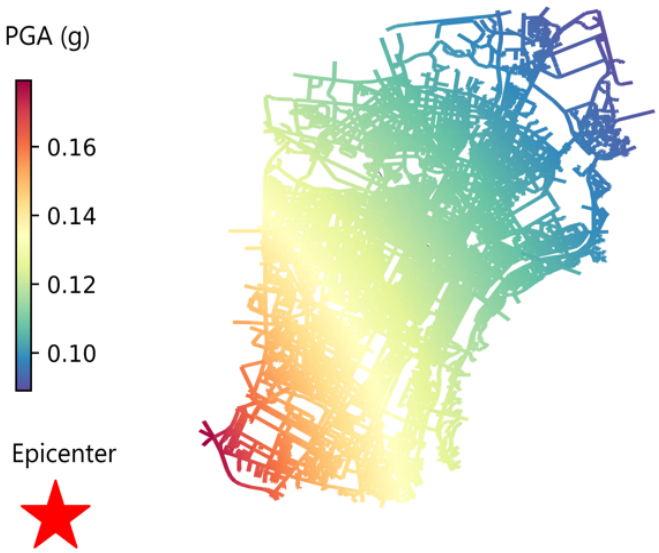

Fig. 7. Earthquake epicentre and Peak Ground Acceleration (PGA).

In addition, an importance factor has been assigned to each pipeline: “2” is assigned to main pipelines, “1.5” to the pipes within the districts, and “1” to the pipes connecting the districts. The number of scenarios is set to 5,000, which yielded an almost normal distribution of the results (

Fig. 8).

Fig. 9 shows the results of a single simulation in terms of water pressure.

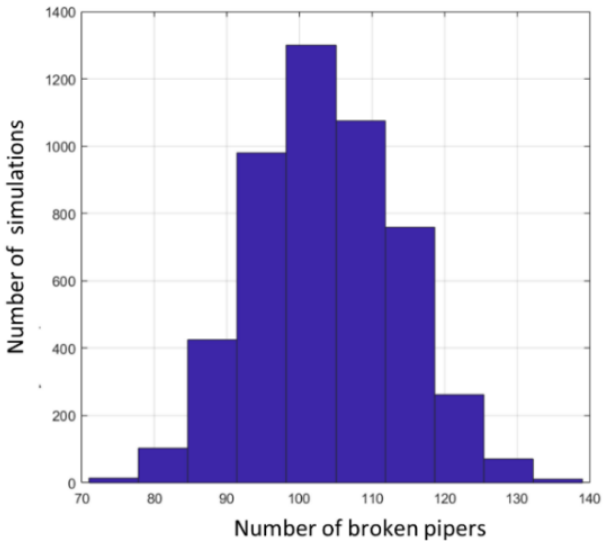

Fig. 8. Histogram of the simulation results. (5,000 simulations, K1= 0.5).

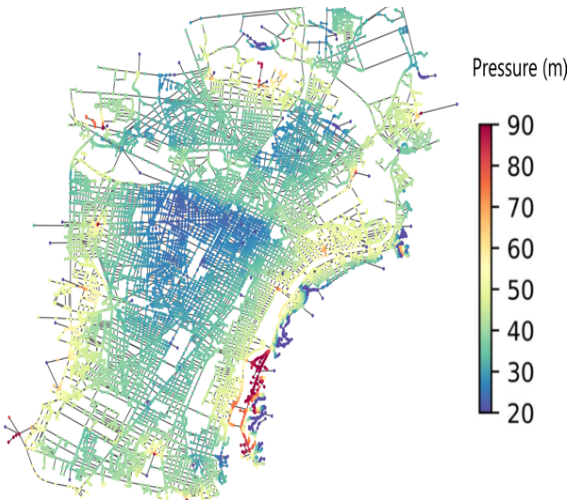

Fig. 9. Water pressure map of one simulation at time step $t=1$ following the event with K1=0.5.

The serviceability functions $F_1(t)$ and $F_2(t)$ are evaluated for the 5,000 simulated scenarios and for three values of $K1$. The simulations considered a random occurrence time of the earthquake. For each simulation, the two resilience indexes are computed using Eq. (3). The results of the resilience indexes at each time step are presented in Fig. 10 in terms of mean value and standard deviation. As can be seen in the figure, pipes with ductile material (low $K1$) show a more resilient behaviour than pipes with fragile material (high low $K1$). The highest resilience indexes correspond to $K1$=0.5.

It is clear that the resilience value follows the water demand pattern: it is lower when damage occurs during high water demand periods. Moreover, from Fig. 10, the resilience index R_2 (referring to the variation of water supply) is more sensitive than the index R_1 (referring to people suffering from water outage).

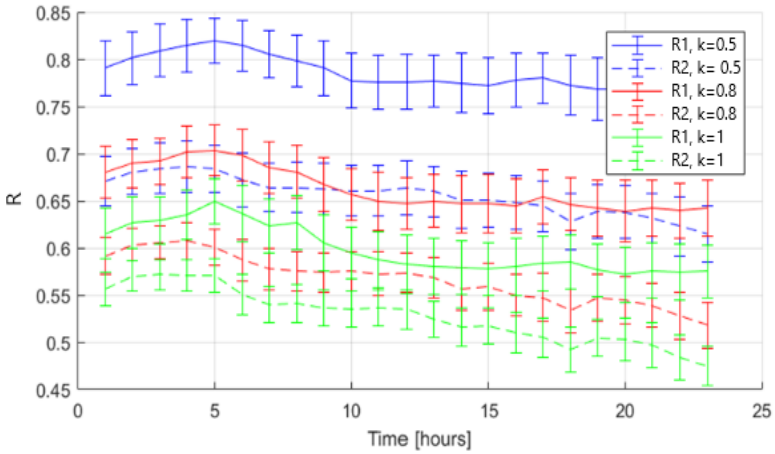

Fig. 10. Resilience indexes R_1 and R_2 for three pipe material values K1.

6. Recovery optimization

Resilience is not only the system's capacity to withstand disruptions but also its rapid recovery capabilities. A holistic approach to resilience, therefore, necessitates a focus on recovery strategies. Here, we introduce a preliminary recovery optimization module to enrich our existing resilience assessment framework.

The ultimate objective of this module is to develop a mathematical optimization model that maximizes the network's serviceability immediately after seismic disruptions. The decision variable in this optimization problem is the set of pipes to be repaired at each time step. Each pipe i in the network is associated with a set of required resources R_i should the pipe need repair. These resources (workers, equipment, costs, etc.) are dependent on the pipe's damage state.

6.1 Objective Function Formulation

The objective function is designed to maximize the rate of improvement in the number of residents being served due to repair work. A resident is considered 'served' if the water pressure at their location is above a specified minimum threshold. This is a time-dependent optimization model where each discrete time step t, an optimization problem is solved with the objective to maximize the number of residents being served given limited resources (i.e., workers, equipment, and budget). This approach enables real-time adjustment based on actual network behavior. Moreover, this approach ensures faster recovery of water service in the immediate aftermath of the disruption, which translates into a higher resilience index after the recovery is completed.

Mathematically, the objective function can be expressed as:

$$\text{Maximize } \Delta S_t \tag{13}$$

where ΔS_t is the number of new served residents at time step t

The objective function *is* subject to constraints that represent the available resources. These constraints can be generically represented as:

$$R_t \leq R_{\max,t} \tag{14}$$

where R_t is a vector that includes the resources used at time step t, and $R_{max,t}$ is the vector representing the maximum available resources at that time step. The elements of R_t could include financial expenditures, manpower allocated, and equipment used, among other things. The constraints ensure that the resources used for recovery at each time step do not exceed their respective available maximums.

Upon the completion of each time step t, the system state is re-evaluated, and a new optimization problem is formulated for the subsequent time step $t+1$. It is important to note that the choice of the optimization objective, which is not to maximize the total water supply but rather to maximize the number of residents being served with adequate water pressure. This decision is predicated on the belief that it is more beneficial to serve a greater number of people with sufficient pressure than to provide fewer people with high pressure, especially in the aftermath of a disruptive event such as an earthquake. The optimization model is currently under development and will be published in subsequent contributions.

7. Conclusions

This study introduces a comprehensive methodology to evaluate and enhance the resilience of Water Distribution Networks (WDNs) in the face of seismic disruptions. Using a virtual city as a test environment, we have developed two key resilience metrics: one for quantifying the number of residents affected by water outages and another for assessing the change in overall water supply. These metrics are evaluated under various earthquake scenarios, factoring in daily water demand and material properties of the pipes, to provide a multi-dimensional view of WDN resilience.

Our model takes into account a range of earthquake scenarios, deploying fragility functions to capture potential damages. These functions consider both the network's characteristics and the seismic forces involved, thus offering a multi-dimensional understanding of WDN resilience. The findings reveal significant correlations between factors such as daily water demand cycles, the timing of seismic events, and the choice of pipe material on overall network resilience.

Furthermore, this paper lays the groundwork for future incorporation of a recovery optimization module, designed to maximize the number of residents being served with adequate water pressure during the recovery process. This module will consider various constraints, including available resources like manpower, equipment, and budget, to prioritize repair tasks dynamically. Future research will focus on the development and integration of this recovery optimization module, adding a dynamic, real-time layer to existing resilience assessments.

References

Bozorgnia, Y., and Bertero, V. V. (2004). *Earthquake engineering: from engineering seismology to performance-based engineering*, CRC press.

Bruneau, M., Chang, S. E., Eguchi, R. T., Lee, G. C., O'Rourke, T. D., Reinhorn, A. M., Shinozuka, M., Tierney, K., Wallace, W. A., and Von Winterfeldt, D. J. E. s. (2003). "A framework to quantitatively assess and enhance the seismic resilience of communities." 19(4), 733-752.

Cimellaro, G. P., Tinebra, A., Renschler, C., and Fragiadakis, M. (2016). "New Resilience Index for Urban Water Distribution Networks." *Journal of Structural Engineering*, 142(8), C4015014.

De Iuliis, M., Kammouh, O., Cimellaro, G. P., and Tesfamariam, S. (2019). "Downtime estimation of building structures using fuzzy logic." *International Journal of Disaster Risk Reduction*, 34, 196-208.

De Iuliis, M., Kammouh, O., Cimellaro, G. P., and Tesfamariam, S. (2020). "Quantifying restoration time of power and telecommunication lifelines after earthquakes using Bayesian belief network model." *Journal of Management in Engineering*.

Eidinger, J. (2001). "Seismic fragility formulations for water systems." *sponsored by the American Lifelines Alliance, G&E Engineering Systems Inc., web site.< http://homepage. mac. com/eidinger*.

Eliades, D. "OpenWaterAnalytics/EPANET-Matlab-Toolkit. https://it.mathworks.com/matlabcentral/fileexchange/25100-openwateranalytics-epanet-matlab-toolkit.".

Ellingwood, B. R., Cutler, H., Gardoni, P., Peacock, W. G., van de Lindt, J. W., and Wang, N. (2016). "The centerville virtual community: A fully integrated decision model of interacting physical and social infrastructure systems." *Sustainable and Resilient Infrastructure*, 1(3-4), 95-107.

ESRI (2011). "ArcGIS Desktop: Release 10. Redlands, CA: Environmental Systems Research Institute.".

Fragiadakis, M., Vamvatsikos, D., and Christodoulou, S. E. "Reliability assessment of urban water networks." *Proc., 15th world conference on earthquake engineering, Lisbon, Portugal*.

Kammouh, O., Cardoni, A., Marasco, S., Cimellaro, G. P., and Mahin, S. (2018a). "Resilience assessment of city-scale transportation networks subject to earthquakes using the Monte Carlo approach." *9th International Conference on Bridge Maintenance, Safety (IABMAS 2018)*, Nigel Powers, Dan M. Frangopol, Riadh Al-Mahaidi, and C. Caprani, eds., CRC Press, Melbourne, Australia, 588.

Kammouh, O., Cimellaro, G. P., and Mahin, S. A. (2018b). "Downtime estimation and analysis of lifelines after an earthquake." *Engineering Structures*, 173, 393-403.

Kammouh, O., Noori, A. Z., Cimellaro, G. P., and Mahin, S. A. (2019). "Resilience Assessment of Urban Communities." *ASCE-ASME Journal of Risk and Uncertainty in Engineering Systems, Part A: Civil Engineering*, 5(1), 04019002.

Kammouh, O., Noori, A. Z., Taurino, V., Mahin, S. A., and Cimellaro, G. P. (2018c). "Deterministic and fuzzy-based methods to evaluate community resilience." *Earthquake Engineering and Engineering Vibration*, 17(2), 261-275.

Marasco, S., Zamani Noori, A., Kammouh, O., Domaneschi, M., Vallero, A., Scutiero, G., and Cimellaro, G. P. (2018). "Seismic Damage Assessment of a Virtual Large-Scale City Model." *9th International Conference on Bridge Maintenance, Safety (IABMAS 2018)*, Nigel Powers, Dan M. Frangopol, Riadh Al-Mahaidi, and C. Caprani, eds., CRC Press, Melbourne, Australia, 588.

Nogal, M., and Honfi, D. (2019). "Assessment of road traffic resilience assuming stochastic user behaviour." *Reliability Engineering and System Safety*, 185, 72-83.

Nogal, M., O'Connor, A., Caulfield, B., and Martinez-Pastor, B. (2016). "Resilience of traffic networks: From perturbation to recovery via a dynamic restricted equilibrium model." *Reliability Engineering and System Safety*, 156, 84-96.

Nogal, M., O'Connor, A., Martinez-Pastor, B., and Caulfield, B. (2017). "Novel probabilistic resilience assessment framework of transportation networks against extreme weather events." *ASCE-ASME Journal of Risk and Uncertainty in Engineering Systems, Part A: Civil Engineering*, 3(3), 04017004.

Pagano, A., Sweetapple, C., Farmani, R., Giordano, R., and Butler, D. (2019). "Water Distribution Networks Resilience Analysis: a Comparison between Graph Theory-Based Approaches and Global Resilience Analysis." *Water Resources Management*, 33(8), 2925-2940.

Soldi, D., Candelieri, A., and Archetti, F. (2015). "Resilience and vulnerability in urban water distribution networks through network theory and hydraulic simulation." *Procedia Engineering*, 119, 1259-1268.

Zamani Noori, A., Marasco, S., Kammouh, O., Domaneschi, M., and Cimellaro, G. (2017). "Smart cities to improve resilience of communities." *8th International Conference on Structural Health Monitoring of Intelligent Infrastructure, SHMII 2017*Brisbane; Australia, 1112-1121.